

Acquisition of Time-Varying Participating Media

Tim Hawkins

Per Einarsson

Paul Debevec

USC Institute for Creative Technologies*



Abstract

We present a technique for capturing time-varying volumetric data of participating media. A laser sheet is swept repeatedly through the volume, and the scattered light is imaged using a high-speed camera. Each sweep of the laser provides a near-simultaneous volume of density values. We demonstrate rendered animations under changing viewpoint and illumination, making use of measured values for the scattering phase function and albedo.

1 Introduction

Very little real world data exists for time-varying volumetric phenomena. We present a technique for capturing density values for particulate scatterers suspended in a flowing fluid, and apply the technique to the capture of smoke. To allow accurate rendering under arbitrary view and illumination, we measure the single-scatter phase function and albedo of the medium.

The basis of our technique is an apparatus that allows a vertical sheet of laser light to be swept horizontally through the volume of interest. We use a high-speed camera to capture the scattered light from these successively illuminated planes. The volume scan can be repeated many times per second to allow the evolution of the volume through time to be captured.

2 Background

In the computer graphics community, several groups [Kass and Miller 1990; Stam 1999; Fedkiw et al. 2001] have demonstrated efficient fluid simulators appropriate for generating realistic smoke motion. [Ihrke and Magnor 2004] captured time-varying volumetric data of a flame using emission tomography from sparse views, using an estimate of the flame silhouette to constrain the solution.

Volumetric datasets are more commonly captured in disciplines such as medicine, atmospheric and oceanic sciences, and fluid dynamics. Medical techniques such as CT and MRI scans acquire volumetric measurements of densities inside the body. In the realm of large scale atmospheric measurements, [Roy and Prevost 1993] scanned cloud density using a lidar scanner. The time profile of back-scattered intensity was very rapidly digitized for many different points, providing a 3D volume of cloud density.

*email:(timh,einarsson,debevec)@ict.usc.edu

In the study of fluid flow and mixing, instantaneous volumetric measurements of concentration and velocity in a fluid flow have been performed. One approach has been to illuminate a gas with a laser sheet or laser line and then image the light scattered from the gas molecules. Scattering from very small particles (individual molecules in this case) is known as Rayleigh scattering. It is very weak, making measurement difficult. Limiting their measurement to points and lines, [Pitts 1993] focussed light to sufficient intensities to measure concentration and velocity in a turbulent flow. [Yip et al. 1986; Yip et al. 1987] performed full planar measurements of Freon 12 concentration in a flow, taking advantage of its strong Rayleigh scattering at the specific wavelength of their laser.

Our approach falls in the category of planar Mie scattering techniques. *Mie scattering* refers to scattering of light from particles much larger than the wavelength of light; smoke falls in this category. Mie scattering is much stronger than Rayleigh scattering, and has been exploited for instantaneous 2D measurements of fluid flow [Anderson et al. 1999; Brummund and Scheel 2000].

Other work has used dyes which fluoresce under specific wavelengths to achieve even higher light levels. This approach, known as laser induced fluorescence (LIF), was used in [Deutsch and Dracos 2001] to measure time-varying 3D concentration of a fluorescent dye in a water jet using a number of different scanning geometries.

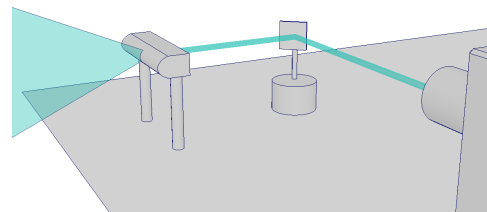


Figure 1: The laser is deflected off a mirror galvanometer and through a cylindrical lens, creating a vertical sheet of light which can be scanned horizontally from side to side.

[Bertocchi et al. 2004] measured the phase function of a cloud of carbon black particles by rotating a photodiode around a laser-illuminated sample. In our work, we measure the phase function with a single photograph using a conical mirror. This approach is similar to that of [Dana and Wang 2004], who used a parabolic mirror to measure outgoing light distributions from surfaces.

3 Data Capture

Our scanning setup is shown in Figure 1. The key components are a laser, a mirror galvanometer, a cylindrical lens, and a high-speed camera (not seen in Figure 1). The galvanometer allows the laser to be scanned back and forth along a horizontal line. After reflecting

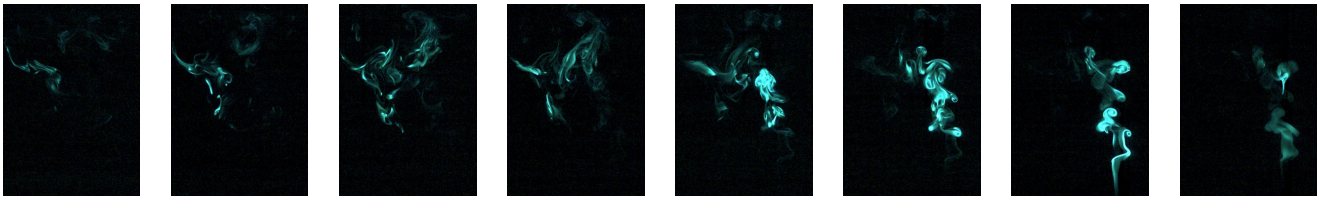


Figure 2: Eight images captured during a single sweep of the laser plane.

off the mirror, the laser is spread into a vertical sheet of light by the cylindrical lens. This sheet of light creates an illuminated plane of smoke, which the camera views from a perpendicular direction.

During scanning, the galvanometer sweeps the laser sheet from the front to the back of the smoke volume, while the camera captures images of the scattered light. The galvanometer then rapidly jumps back to the front of the smoke volume and the process is repeated. In this work we capture 200 images during each volume scan. At 5000 frames per second, this allows the volume to be scanned at 25 Hz. We placed both the camera and galvanometer 3 meters from the working volume, and chose the camera lens, cylindrical lens, and galvanometer scan angle so that the camera field of view and laser frustum were both 6° . This provided a working volume of approximately $30 \times 30 \times 30$ cm.

The galvanometer control software also triggers the camera, allowing the frame capture to be synchronized with the position of the laser slice. This assures that corresponding slices in successive captured volumes are sampled at the same position.

The high frame rate and the small fraction of the total light scattered to the camera require a relatively powerful laser. We use an argon ion laser that produces 3 watts of light at a set of wavelengths closely clustered around 500 nm.

3.1 Calibration

Interpreting the image data as a density field requires knowing the geometry and radiometry of the camera and lighting setup. We use a planar checkerboard pattern to calibrate the pose and intrinsic parameters of the camera using the technique of [Zhang 2000].



Figure 3: (a) Filter with horizontal lines used for characterizing light volume. (b) Captured image of laser through filter.

We calibrate the position and intensity of the laser, as well as the position of the sequential laser planes P_s , by placing a pattern of horizontal lines between the cylindrical lens and the working volume. This changes the vertical slice of light into a series of dots. We then place a checkerboard at an angle such that it is illuminated by the laser and also visible to the camera. Because the position of the checkerboard is determined by the camera calibration procedure, we can then determine the position of a given dot of light in a given frame corresponding to one position of the laser slice. Moving the checkerboard to another position allows the same dot of light to be observed at a different 3D position. Connecting these dots then gives a line which passes through the nodal point L_c of

the laser scanner. Repeating this for another dot gives another such line, and intersecting the two lines determines L_c .

Similarly, any two identified points on the laser line for a given slice s , together with L_c , determines the plane P_s of illumination.

We observed that the intensity of illumination varied as a function of slice s and of elevation angle ϕ within each laser slice. To correct for this, we placed a uniform diffuse plane at an angle where it was visible to both the laser and the camera and captured a sequence of frames. As the laser scans this reflectance standard, the observed intensities are directly proportional to the intensity of laser light for each laser plane and pixel position. Having calibrated the laser planes P_s and the camera position, we can find the 3D point v corresponding to each laser plane and pixel position, and apply the appropriate intensity compensation when computing densities along the ray from the laser position L_c through the point v . Although this corrects for the relative intensity differences across the laser frustum, we should note that we do not measure the absolute intensity of the laser. The resulting density fields are therefore only recovered up to an unknown scale factor.

We have assumed that image intensity values can be directly interpreted as density values. This assumes that the effects of extinction and multiple scattering within the volume are negligible. Although we found that this assumption held for the smoke volumes we captured, this assumption will fail when the densities become very high such as for thick smoke or dyes in water, or when the scattering volume becomes large.

4 Measuring scattering parameters

To render a captured density volume accurately, we must also know the basic scattering characteristics of the medium. In particular we must know the *phase function*, which describes the angular distribution of scattered light, and the *albedo*, which describes the tendency of the medium to scatter light rather than absorb it.

To measure these quantities, we use the setup shown in Figure 4. Smoke is confined within a transparent tank. A fan circulates the air to maintain homogeneity. A spherical glass observation chamber is added at the top.

4.1 Phase Function

The phase function of a scattering medium describes the distribution of outgoing scattered light per scattering event. It is assumed to be a function only of the angle between the direction of the incoming light and the direction of scattered light, or *phase angle*.

We developed a novel apparatus to measure the phase function from a single photograph. We first fill the tank and observation chamber with smoke. Relatively thin smoke is used to minimize the effect of multiple scattering. We then direct the laser beam through the spherical observation chamber. A strip of a 45 degree conical mirror encircles the observation chamber, as seen in Figure 5(a). Two small holes are drilled through the conical mirror to allow the laser to pass through it into the observation chamber, and to exit without creating unwanted reflections or stray light.

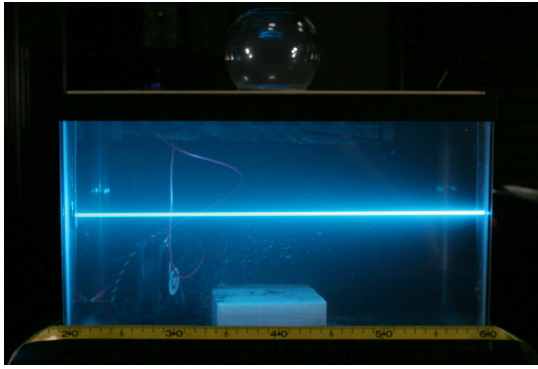


Figure 4: Setup for measuring phase function and albedo. For phase function measurement, the laser is directed through the spherical chamber on top. For albedo measurement the laser enters the lower tank, as shown here.

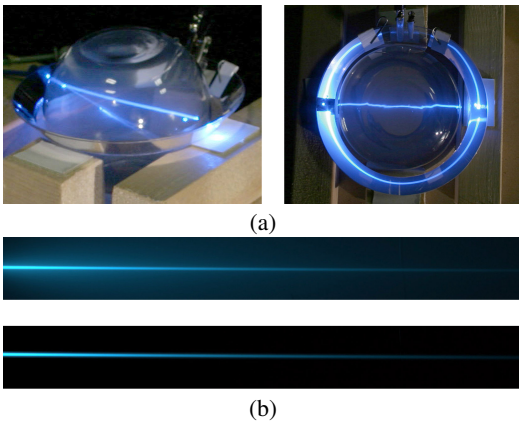


Figure 5: (a) Two views of the phase function capture setup. From above the conical mirror reflects light coming from the center of the laser line, creating a circle of light that captures all excitant directions. (b) Original extinction image (top) and extinction image with effect of multiple scattering removed (bottom).

When imaged from above, the conical mirror allows the light scattered from the center of the observation chamber to be seen simultaneously from all directions. An example of such an image is shown on the right in Figure 5(a). We capture a high dynamic range image of this area and find the image intensities corresponding to each outgoing angle.

The normalized phase function is derived from the observed intensities $I(\theta)$ by first scaling all observations by $\sin(\theta)$ to correct for foreshortening of the laser line, and then normalizing this quantity to have integral 4π over the sphere of outgoing directions:

$$\Phi(\theta) = \frac{2I(\theta)\sin(\theta)}{\int_0^\pi I(\theta)\sin(\theta) \cdot \sin(\theta)d\theta} \quad (1)$$

The measured phase function can be seen in Figure 6. It exhibits the strong forward scattering common to many scattering media.

4.2 Albedo

The albedo of a scattering medium is defined as the ratio of scattered light to the sum of scattered light and absorbed light.

Given the known phase function, the albedo may be measured using the simple setup illustrated in Figure 4. To assure the rate

of extinction is easily observable, a high smoke density is used. The laser beam is directed through the tank and a high dynamic range image is captured, as shown in Figure 5(b). The effects of multiple scattering along the imaged laser line are removed at each horizontal position by subtracting the average of a small window of pixels above and below the laser line.

To compute the albedo we measure the intensity L_i of the laser from a diffuse reflectance standard oriented at 45° to both the camera and the laser. If the phase function were isotropic and all of the light extinction were due to scattering, the light intensity L_s scattered from the smoke at 90° as measured by a camera pixel is:

$$L_s = \frac{\sqrt{2}L_i k}{4} \quad (2)$$

where k is the observed fractional extinction per pixel, and the factor of $\sqrt{2}/4$ accounts for the greater than isotropic efficiency of the diffuse reflector at a 45° exitant angle. Accounting for the known phase function, we then compute the albedo as:

$$\omega = \frac{4L_s}{\sqrt{2}L_i k \Phi(90)} \quad (3)$$

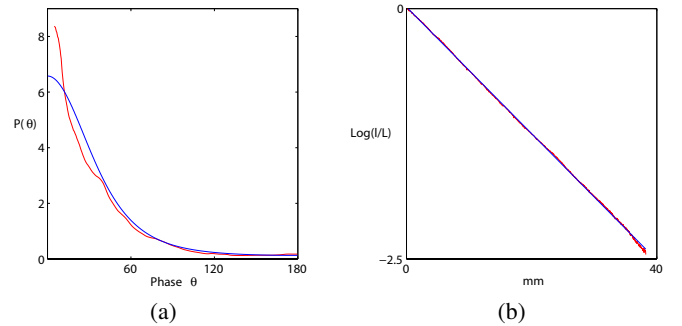


Figure 6: (a) Measured phase function (red) with best-fit Henyey-Greenstein lobe ($g=0.32$) (blue). (b) Log-linear plot, showing the expected exponential decay of light intensity. In this case, 8.7% of the light is scattered or absorbed per centimeter.

5 Results

We visualize our time-varying data sets using a Monte Carlo ray tracing renderer. A data set typically consists of approximately 120 volumes, each with a resolution of $640 \times 480 \times 200$. We store the recovered density values in voxel grids, and for each frame we use ray marching to step through the volume along the camera rays. At each step we interpolate the volume's density and sample the incident illumination to compute the amount of being light scattered towards the camera, as well as the attenuation due to extinction. Here, we use our measured values for albedo and phase function to accurately determine the ratio of scattered to absorbed light and the angular distribution of the scattered light. For renderings using environmental illumination, we sample the incident light intensity using an importance sampling algorithm based on [Pharr and Humphreys 2004].

Figure 7 shows three renderings of captured smoke volumes under novel viewpoints and illumination. To make the smoke more easily visible, the scale factor for the recovered smoke density has been chosen to be significantly higher than for the actual smoke. The measured albedo for this smoke was 0.62. We are also able to change the appearance of the smoke by modifying the albedo, extinction and phase function. Examples of such renderings are included on the accompanying video.

6 Conclusion

We have presented a technique for capturing time-varying density of participating media, and demonstrated its application to the capture of smoke. We have also demonstrated realistic renderings making use of measured scattering parameters for the medium.

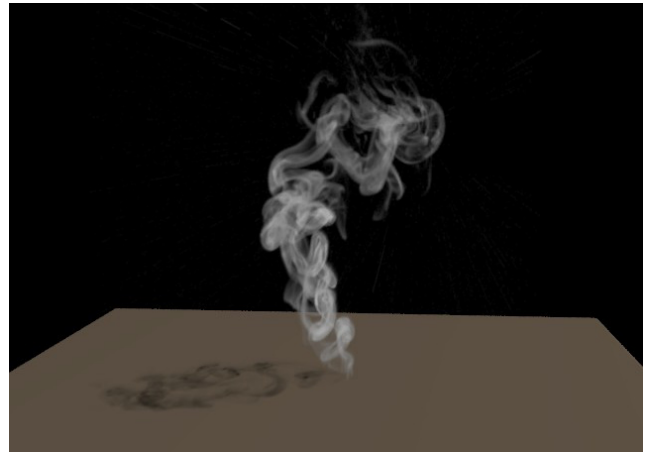
For future work, compensating for the effects of extinction and multiple scattering would improve accuracy for large volumes or when the density of scatterers is high. Such compensation should be possible when the total attenuation from extinction and blurring from multiple scattering are not excessive.

7 Acknowledgements

We gratefully acknowledge Martin Gundersen for use of the ion laser, and Andrew Jones for his graphic design work and video editing. The project or effort described here has been sponsored by the U.S. Army Research, Development, and Engineering Command (RDECOM). Statements and opinions expressed do not necessarily reflect the position or the policy of the United States Government, and no official endorsement should be inferred.

References

- ANDERSON, M., PURANIK, B., OAKLEY, J., PETERSON, R., AND BONAZZA, R. 1999. Planar imaging of density interfaces accelerated by strong shocks. In *22nd International Symposium on Shock Waves*.
- BERTOCCHI, R., KRIBUS, A., AND KARNI, J. 2004. Experimentally determined optical properties of a polydisperse carbon black cloud for a solar particle receiver. *Journal of Solar Energy Engineering* 126 (August), 833–841.
- BRUMMUND, U., AND SCHEEL, F. 2000. Characterization of a supersonic flow-field using different laser based techniques. In *10th International Symposium on Applications of Laser Techniques to Fluid Mechanics*.
- DANA, K., AND WANG, J. 2004. Device for convenient measurement of spatially varying bidirectional reflectance. *Journal of the Optical Society of America A* 21, 1 (January), 1–11.
- DEUSCH, S., AND DRACOS, T. 2001. Time resolved 3d passive scalar concentration-field imaging by laser induced fluorescence in moving liquids. *Measurement Science and Technology* 12, 188–200.
- FEDKIW, R., STAM, J., AND JENSEN, H. W. 2001. Visual simulation of smoke. In *SIGGRAPH '01: Proceedings of the 28th annual conference on Computer graphics and interactive techniques*, ACM Press, 15–22.
- IHRKE, I., AND MAGNOR, M. 2004. Image-based tomographic reconstruction of flames. In *Proc. ACM/EG Symposium on Animation*, 367–375.
- KASS, M., AND MILLER, G. 1990. Rapid, stable fluid dynamics for computer graphics. In *SIGGRAPH '90: Proceedings of the 17th annual conference on Computer graphics and interactive techniques*, ACM Press, 49–57.
- PHARR, M., AND HUMPHREYS, G. 2004. Improved infinite area light source sampling. <http://pbrt.org/plugins.php>.
- PITTS, W. 1993. Rayleigh light scattering studies of turbulent mixing. In *Combustion Institute/Eastern States Section. Chemical and Physical Processes in Combustion. Fall Technical Meeting*, 8–16.
- ROY, G., AND PREVOST, D. 1993. Sampling with scanning lidar systems. *Measurement Science and Technology* 4, 204–214.
- STAM, J. 1999. Stable fluids. In *SIGGRAPH '99: Proceedings of the 26th annual conference on Computer graphics and interactive techniques*, ACM Press/Addison-Wesley Publishing Co., 121–128.
- YIP, B., FOURGUETTE, D. C., AND LONG, M. B. 1986. Three-dimensional gas concentration and gradient measurements in a photoacoustically perturbed jet. *Applied Optics* 25, 21 (November), 3919–3922.
- YIP, B., LAM, J. K., WINTER, M., AND LONG, M. B. 1987. Time resolved three-dimensional concentration measurements in a gas jet. *Science* 235, 4793 (March), 1209–1211.
- ZHANG, Z. 2000. A flexible new technique for camera calibration. In *IEEE Transactions on Pattern Analysis and Machine Intelligence*, vol. 22, 1330–1334.



(a)



(b)



(c)

Figure 7: (a) A captured smoke volume rendered with a point light. (b) The same smoke volume rendered with two spotlights of different colors. (c) A smoke volume rendered with environmental illumination.